AFRL-RD-PS-
TN-2011-0045

AFRL-RD-PS-
TN-2011-0045

COHERENT BEAM COMBINING ELEMENT FOR FIVE 150-W FIBER LASERS BY VOLUME BRAGG GRATINGS IN PTR GLASS

Leonid Glebov

03 August 2011

Technical Note

APPROVED FOR PUBLIC RELEASE; DISTRIBUTION IS UNLIMITED.

AIR FORCE RESEARCH LABORATORY
Directed Energy Directorate
3550 Aberdeen Ave SE
AIR FORCE MATERIEL COMMAND
KIRTLAND AIR FORCE BASE, NM 87117-5776

Report Documentation Page

Form Approved
OMB No. 0704-0188

1. REPORT DATE	2. REPORT TYPE	3. DATES COVERED
03 AUG 2011		

4. TITLE AND SUBTITLE
Coherent Beam Combining Element for Five 150-W Fiber Lasers by Volume Bragg Gratings in PTR Glass

5a. CONTRACT NUMBER
FA9451-10-C-0253

5b. GRANT NUMBER

5c. PROGRAM ELEMENT NUMBER
62605F

6. AUTHOR(S)
Leonid Glebov

5d. PROJECT NUMBER
4866

5e. TASK NUMBER
LR

5f. WORK UNIT NUMBER
DF702211

7. PERFORMING ORGANIZATION NAME(S) AND ADDRESS(ES)
Optigrate Corporation,3267 Progress Dr.,Orlando,FL,32826-3230

8. PERFORMING ORGANIZATION REPORT NUMBER

9. SPONSORING/MONITORING AGENCY NAME(S) AND ADDRESS(ES)

10. SPONSOR/MONITOR'S ACRONYM(S)

11. SPONSOR/MONITOR'S REPORT NUMBER(S)

12. DISTRIBUTION/AVAILABILITY STATEMENT
Approved for public release; distribution unlimited.

13. SUPPLEMENTARY NOTES
The original document contains color images.

14. ABSTRACT
A compact beam combiner based on multiplexed volume Bragg gratings (VBGs) recorded in photo-thermo-refractive (PTR) glass was demonstrated. This element was designed to provide efficient superposition of 5 coherent beams from 150 W fiber amplifiers operating at the testbed developed at AFRL (KAFB). Five VBGs were multiplexed in a PTR glass wafer in such a way that they have common (degenerate) Bragg angle. Thus it will take the 5 beams which are incident from 5 different angles and superimpose the 5 beams on top of each other in space and the direction that correspond to a common Bragg angle. In contrary, when it is illuminated by a single laser beam from the opposite direction, it split this beam into 5-channels.

15. SUBJECT TERMS

16. SECURITY CLASSIFICATION OF:			17. LIMITATION OF ABSTRACT	18. NUMBER OF PAGES	19a. NAME OF RESPONSIBLE PERSON
a. REPORT	b. ABSTRACT	c. THIS PAGE			
unclassified	**unclassified**	**unclassified**		**28**	

NOTICE AND SIGNATURE PAGE

AFRL-RD-PS-TN-2011-0045 HAS BEEN REVIEWED AND IS APPROVED FOR PUBLICATION IN ACCORDANCE WITH ASSIGNED DISTRIBUTION STATEMENT.

Leanne J. Henry

LEANNE HENRY, DR-III
Project Officer

Eugene J Bednarz

EUGUENE J. BEDNARZ, DR-IV, DAF
Chief, Laser Division

REPORT DOCUMENTATION PAGE

Form Approved
OMB No. 0704-0188

1. REPORT DATE *(DD-MM-YYYY)* 03-08-2011	**2. REPORT TYPE** Technical Note	**3. DATES COVERED *(From - To)*** 19 May 2010- 03 Aug 2011
4. TITLE AND SUBTITLE Coherent Beam Combining Element for Five 150-W Fiber Lasers by Volume Bragg Gratings in PTR Glass		**5a. CONTRACT NUMBER** FA9451-10-C-0253
		5b. GRANT NUMBER
		5c. PROGRAM ELEMENT NUMBER 62605F
6. AUTHOR(S) Leonid Glebov		**5d. PROJECT NUMBER** 4866
		5e. TASK NUMBER LR
		5f. WORK UNIT NUMBER DF702211
7. PERFORMING ORGANIZATION NAME(S) AND ADDRESS(ES) Optigrate Corporation 3267 Progress Dr. Orlando, FL 32826-3230		**8. PERFORMING ORGANIZATION REPORT NUMBER**
9. SPONSORING / MONITORING AGENCY NAME(S) AND ADDRESS(ES) Air Force Research Laboratory 3550 Aberdeen Avenue SE Kirtland AFB, NM 87117-5776		**10. SPONSOR/MONITOR'S ACRONYM(S)** AFRL/RDLA
		11. SPONSOR/MONITOR'S REPORT NUMBER(S) AFRL-RD-PS-TN-2011-0045

12. DISTRIBUTION / AVAILABILITY STATEMENT

Approved for public release; distribution unlimited. "Government Purpose Rights"

13. SUPPLEMENTARY NOTES

377ABW-2011-1194; August 11, 2011.

14. ABSTRACT: A compact beam combiner based on multiplexed volume Bragg gratings (VBGs) recorded in photo-thermo-refractive (PTR) glass was demonstrated. This element was designed to provide efficient superposition of 5 coherent beams from 150 W fiber amplifiers operating at the testbed developed at AFRL (KAFB). Five VBGs were multiplexed in a PTR glass wafer in such a way that they have common (degenerate) Bragg angle. Thus it will take the 5 beams which are incident from 5 different angles and superimpose the 5 beams on top of each other in space and the direction that correspond to a common Bragg angle. In contrary, when it is illuminated by a single laser beam from the opposite direction, it split this beam into 5-channels.

15. SUBJECT TERMS

Coherent beam combiner, volume Bragg grating, photo-thermo-refractive (PTR) glass

16. SECURITY CLASSIFICATION OF:			**17. LIMITATION OF ABSTRACT**	**18. NUMBER OF PAGES**	**19a. NAME OF RESPONSIBLE PERSON** Leanne Henry
a. REPORT Unclassified	**b. ABSTRACT** Unclassified	**c. THIS PAGE** Unclassified	SAR	28	**19b. TELEPHONE NUMBER *(include area code)*** 505-846-9302

Standard Form 298 (Rev. 8-98)
Prescribed by ANSI Std. 239.18

This page is intentionally left blank.

TABLE OF CONTENTS

Section	Page
List of Figures……………………………………………………………………..	iii
List of Tables………………………………………………………………………	iv
1. SUMMARY……………………………………………………………………..	1
2. INTRODUCTION……………………………………………………………	2
3. METHODS, ASSUMPTIONS AND PROCEDURES………………………….	10
4. RESULTS AND DISCUSSION…………………………………………………	12
5. CONCLUSIONS………………………………………………………………	17
6. RECOMMENDATIONS………………………………………………………...	18
7. REFERENCES………………………………………………………………..	19

LIST OF FIGURES

Figure **Page**

1 Absorption spectrum of typical PTR glass……………………………………….. 3
2 Optical scheme of coherent coupling of laser diodes. a) combining of independent diodes, b) spectral locking of LD-1, c) spectral locking of LD 1 and phase locking of two diodes, d) phase locking of two diodes….……………….…………….. 4
3 Emission spectra of laser diodes. A) low resolution, light curve-- original diode, dark curve—the same diode with a locking grating as an output coupler, b) high resolution, dark curve—LD-1 locked by a locking grating, light curve—LD-2 locked by a coupling gratings………… ………………………………………. 5
4 Interference pattern produced by the beams of two laser diodes. A) isolated diodes, b) diodes coupled by a narrow- band PTR Bragg grating……..………………….… 5
5 Three-channel array of grating coupled surface emitting lasers (GCSELs) coupled by a striped reflecting volume Bragg grating (VBG)……………………………………………………………………….. 7
6 Far field emission of a three-channel array……………………….................... 7
7 Experimental setup for coherently locking two fiber lasers with a Beam splitting VBG in the symmetrical configuration. L1, L2, L3, L4: f=8 mm 0.5 NA aspheric lens; BS beam splitter; PD: 915 nm pump diodes; PSC: (6+1)x1 pump-signal combiner……………………………….………….....……....8
8 Multiplexed VBG beam splitter. (A) 1:2 M-VBG splitter. (B) 1:4 M-VBG splitter. (C) 1:8 M-VBG splitter………..……………..……………………………… 9
9 (left) Emission spectra (limited by the spectrometer resolution) and (right) fringe pattern of the two channels for Coherent locking using 2nd order MVBG...……… 10
10 Schematic of the holographic recording setup. He-Cd – UV laser at 325 nm, M – mirrors, D – diaphragms, L – lenses, PP – plane-parallel plates, S – screen, BS – beam splitter, PT – glass sample, TP – object projecting mirror, He-Ne – Vis laser at 633 nm.…………………..…….………………………….………….. 10
11 Angular profile of multiplexed Bragg grating…………………………………….. 14
12 Intensity distribution of each of the split beams…………………………………… 14
13 Optical setup for the measurement of the phase shift induced by Laser heating in an optical flat. W: wedge, L: lens, D: diaphragm, D_i: detector, M: mirror, C: chopper, and BD: beam dumps…………………………..…….. 15

LIST OF TABLES

Table		Page
1	Parameters of the first prototype in beam splitting mode………………………..	12
2	Parameters of the second prototype in beam splitting mode…………………….	13
3	Measured absorption in the N36-39 multiplexed VBG at 1085…………………	16

1. SUMMARY

The objective of this project was a demonstration of a compact beam combiner based on multiplexed volume Bragg gratings (VBGs) recorded in photo-thermo-refractive (PTR) glass. This element was designed to provide efficient superposition in the near and far fields of five coherent beams from 150 W fiber amplifiers operating in the testbed developed at AFRL Kirtland AFB, NM. Five VBGs were multiplexed in a PTR glass wafer in such a way that they had a common (degenerate) Bragg angle at the specified wavelength of 1064 nm. The combiner will thus take five properly phased beams which are incident from 5 different angles and superimpose the five beams on top of each other in space with a direction that corresponds to a common Bragg angle. In contrary, when the combiner is illuminated by a single laser beam from the opposite direction (common Bragg angle) the beam will be split into 5 channels with equal power.

2. INTRODUCTION

Recent advances in solid-state, fiber, and diode laser technologies, along with various beam combination techniques have resulted in a rapid increase in the output power available from these devices. The design of high power laser systems exceeding the limits of single-aperture emitters relies on coherent and incoherent combination of radiation from multiple emitters into a single beam with enhanced brightness. Coherent combination requires mutual phase locking of multiple emitters. Therefore, coherent oscillation of a multi-channel laser system requires conversion of all emitters to a single-frequency regime (single transverse and single longitudinal mode) and precise control of the relative phases of all emitters. There are several approaches to mode selection and phase locking. The utilization of volume Bragg gratings (VBGs) for coherent beam combining was recently surveyed in Ref. [1].

The most critical parameters of a high power laser system for the determination of both low divergence and portability are efficiency and brightness. A low efficiency laser system generates an excessive amount of heat during operation. Maintenance of a low beam divergence (high brightness) under heat loading while providing efficient heat dissipation in a portable system are the main challenges associated with high power laser systems. Semiconductor lasers are the highest efficiency laser sources demonstrated to date. A number of manufacturers have developed high power laser diodes with efficiencies exceeding 70% [2-4]. However, poor beam quality and high divergence of high power diode laser systems prevents their use as primary sources of emission in a number of important applications. Diodes have been used extensively to pump other lasers, particularly solid state and fiber lasers, capable of producing high-quality beams at the expense of reduced output power and overall system efficiency. Diode-pumped solid state and fiber lasers are essentially brightness converters for diode laser systems, providing enhanced brightness at the expense of overall system efficiency. While this approach has proved very useful and high efficiency of conversion has been achieved, nonlinear effects have limited the maximum output power achievable for a single system. Because of this, the main approach for a further increase in the brightness of laser systems is beam combining. VBGs which are expected to work as multichannel beam splitters or combiners have several advantages in comparison to conventional beam splitters. One advantage is a high laser damage threshold which makes multichannel beam combining in a single element within a polished glass plate without complex surface relief possible.

We propose a design architecture for a high power laser system where the final stage is a multi-channel beam combiner which forms a single beam having enhanced brightness from a number of coherent emitters impinging at different angles on the beam combiner. Each coherent emitter is a single-transverse-mode semiconductor, solid state or fiber laser. Coherent coupling, spectral stabilization and transverse mode selection are performed by VBGs recorded in photo-thermal refractive (PTR) glass [5].

PTR glass is a Na_2O-ZnO-Al_2O_3-SiO_2 material doped with silver, cerium, and fluorine. A permanent refractive index change in PTR glass occurs after exposure to ultraviolet (UV) radiation followed by thermal development. While being photo-sensitive in the UV, PTR glass offers high transmittance in the near-infrared (IR) and visible parts of spectrum (350-2700 nm transparency window, Fig. 1, with an absorption in the near-IR region of about 10^{-4} cm^{-1}. The history of the study of the photo-thermo-refractive process and its parameters from the point of view of hologram recording are summarized in surveys [6,7].

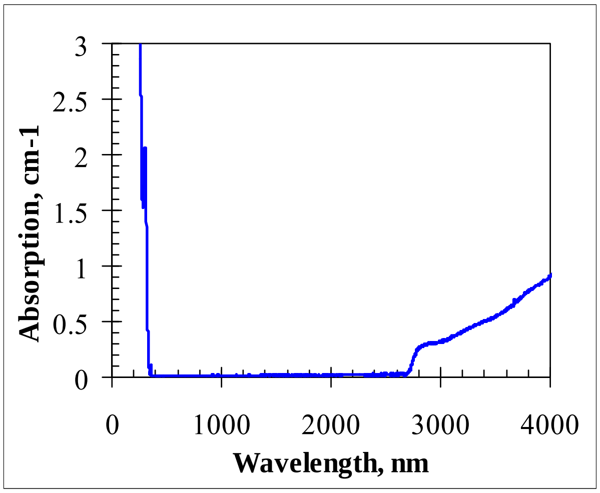

Fig. 1. Absorption spectrum of typical PTR glass.

Recent improvements in PTR technology have resulted in the creation of volume phase holograms (Bragg gratings) having low losses and an extremely high diffraction efficiency exceeding 99% [8,9]. PTR glass has excellent thermo-mechanical properties to include thermal stability of a hologram up to 400°C, a refractive index practically independent of temperature ($dn/dT=5\times10^{-7}\ K^{-1}$), a coefficient of thermal expansion of 8.5×10^{-6}/K, and a thermal conductivity of 0.01 W/cm-K. A laser damage threshold of 40 J/cm^2 for 8 ns pulses, and a tolerance of continuous wave (CW) laser radiation in the near IR region to at least several tens of kilowatts per square centimeter, make PTR-glass holograms attractive for high-power laser applications.

A volume holographic optical element is an interference pattern recorded in a volume photosensitive medium by means of a spatial refractive index modulation. Such elements produce a transformation of optical beams due to diffraction of the propagating wave by the modified refractive index. The simplest volume holographic element is a volume Bragg grating which is a system of planar layers having a modified refractive index. Depending on the diffraction angle and the orientation of a grating in the plate, one can distinguish both transmitting and reflecting Bragg gratings. Angular selectivity of transmitting VBGs becomes narrower with an increase in spatial frequency and thickness of the grating. For a grating with a thickness of several millimeters in PTR glass [10], variation of the spatial frequency can provide angular selectivity ranging from about 0.1 to several mrads. Spectral selectivity of transmitting VBGs can vary from several tens of nanometers down to the sub-nm range. Reflecting VBGs can have deflection angles from 120 to 180°, angular selectivity from 1 to 100 mrad, and spectral selectivity from 0.01 to 2 nm.

VBGs recorded in PTR glass have found multiple applications in different areas of lasers and photonics. This report is dedicated to one of those applications which is phase locking of lasers through coherent beam combining.

Increasing the brightness of lasers by coherent coupling of multichannel emitters has been intensely studied for more than 25 years and has been published in numerous papers (see one of the recent surveys [11]). There are two basic approaches for coherent coupling. The first one is to inject coherent radiation into separate lasers forcing them to emit coherently [12-16]. This approach enables oscillation of all components of the system in the same mode. However, changes in the refractive index of gain materials under strong pumping results in phase mismatch between different channels. Therefore, the problem of precise phase measurement and control of all channels is the main challenge associated with this approach. The second approach is to design a multichannel resonator enabling coherent emission of all its components. This approach is described in numerous publications [17-20]. Although phase control of the channels is avoided, a stable and efficient coupling is prevented by the tendency of a multichannel system to switch between the different modes of a complex resonator. Although a number of dispersive elements have been used to eliminate multimode oscillation, stable coherent coupling at high levels of pumping has not been reported. Recently, narrow-band volume Bragg gratings have been used to create extremely dispersive external resonators for laser diodes supporting only one mode. In addition, use of the same grating for coupling of multiple diodes has resulted in the stable coherent coupling of laser diodes [1, 21].

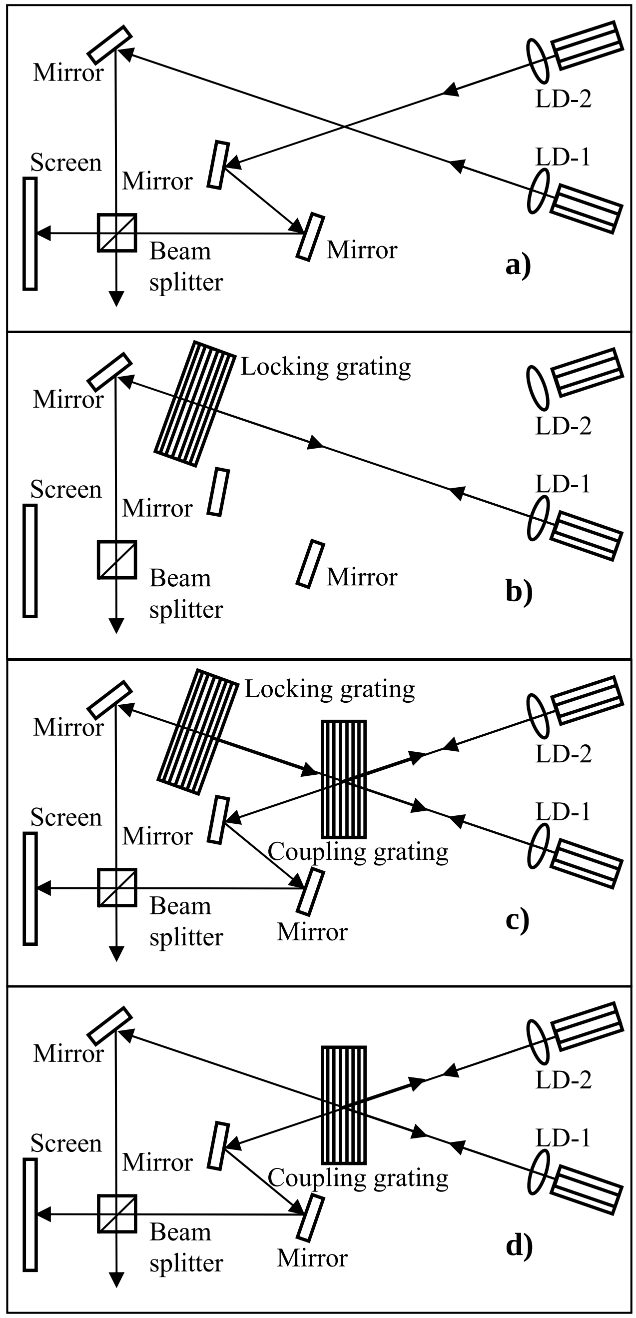

Fig. 2. Optical scheme of coherent coupling of laser diodes: a) – combining of independent diodes, b) – spectral locking of LD-1, c) – spectral locking of LD-1 and phase locking of two diodes, d) phase locking of two diodes.

The experimental setup for coherent coupling and observation of an interference pattern between two semiconductor laser diodes is shown in Fig. 2. Two commercial single-transverse-mode 50 mW laser diodes with standard antireflection coatings (~5%) emitting collimated beams in the 980 nm range were used. They were placed on separate stages mounted on the same vibration isolated optical table (Fig. 2a). The optical axes of the diodes were about 10 cm above the surface of the table and the distance between the diodes was about 2 cm. Emission spectra of the diodes consisted of several fluctuating lines of about 3.5 nm total spectral width (Fig. 3a). The laser outputs were combined on a screen by a system of mirrors and a beam splitter (Fig. 2a). Since these lasers were not coherent, the combined beam manifested itself as a typical speckle pattern (Fig. 4a).

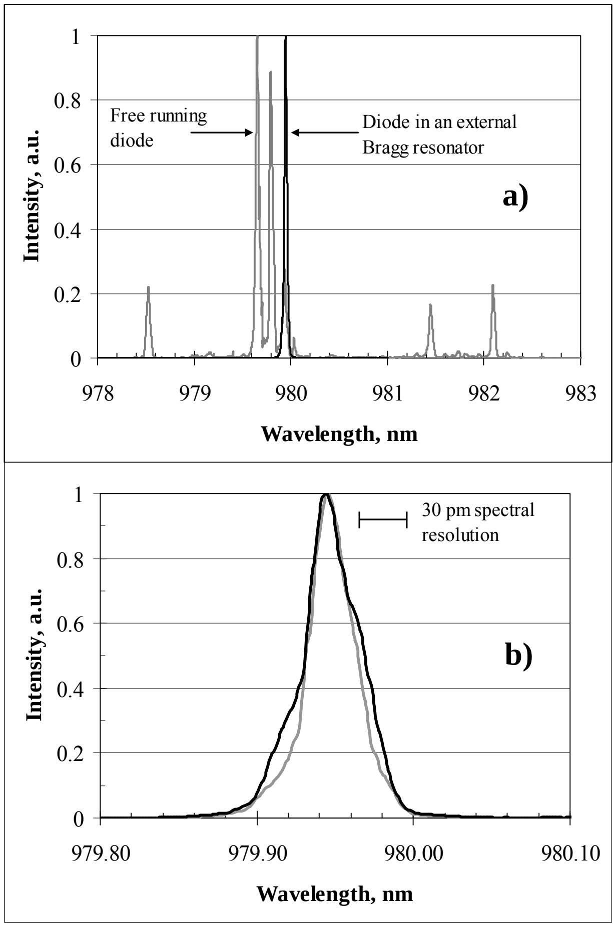

Fig. 3. Emission spectra of laser diodes: a) – low resolution, light curve – original diode, dark curve – the same diode with a locking grating as an output coupler; b) – high resolution, dark curve – LD-1 locked by a locking grating, light curve – LD-2 locked by a coupling gratings.

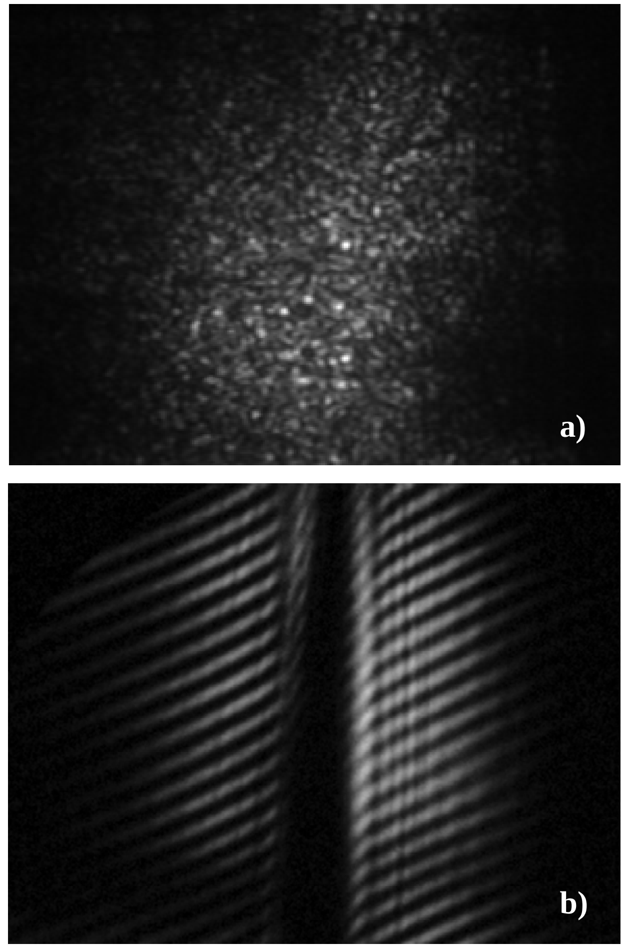

Fig. 4. Interference pattern produced by the beams of two laser diodes: a) – isolated diodes, b) – diodes coupled by a narrow-band PTR Bragg grating.

A number of PTR Bragg gratings, each having a spectral selectivity narrower than 100 pm, half width to the first zero (HWFZ), and a reflection coefficient of 98% for a plane monochromatic wave were used to enable phase locking of the two diodes. First, a locking grating working in a retroreflecting mode at 979.97 nm, was placed in the beam of laser diode LD-1 (Fig. 2b) to cause spectral narrowing of the laser from several nanometers to less than 30 pm (Fig. 3b), i.e., the spectral resolution of the optical spectrum analyzer. Second, a coupling grating was placed in the beam of LD-1 and aligned to provide efficient diffraction of the narrow-band emission at 979.97 nm from LD-1 to LD-2, thereby coupling these two lasers (Fig. 2c). The result was that both lasers emitted narrow lines separated by less than 150 pm. Because there was no phase locking from the spectral locking of the laser diodes, the combined beam produced from the coupled narrow band lasers was still a fluctuating speckle pattern similar to that shown in Fig.

4a. After the locking grating was removed from the resonator of LD-1 (Fig. 2d), wide-band emission of the two laser diodes was observed similar to that seen with the geometry in Fig. 2a.

However, it was found that in the case where the spectral width of the coupling grating (~40 pm HWFZ) was less than the axial mode separation of the internal resonator (~70 pm) of the laser diodes, locking of the lasers in Fig 2c to the same frequency and phase was achieved by tuning the pumping current. In this case, the emission spectrum of both lasers was identical (Fig. 3b). When these two beams were combined, the interference pattern shown in Fig. 4b (the dark and light lines at 45 degrees) was produced. With the above coupling grating in place, the locking grating could be removed from resonator (Fig. 2d) while still maintaining a spectral width of radiation from both diodes below 30 pm as well as the interference pattern. The fact the interference pattern was stable for a long period of time was remarkable considering that the diodes and the coupling grating were mounted on three different stages resulting in a resonator length of 15 cm. It is important to note that coherent coupling was observed at high levels of pumping, i.e., at 5 times above the threshold. Coherent coupling was not continuously stable as the current was increased from the threshold to the nominal value for a fixed temperature of diodes. However, for any fixed current, coherent coupling could be achieved by fine tuning the temperature of diodes. The total power of the coherent radiation from the coupled lasers was above 80 mW, corresponding to more than 80% of the total power of the independent lasers.

The black stripe in the middle of the interference pattern in Fig. 4b appears for the configuration shown in Fig. 2d and corresponds to the angle having the highest diffraction efficiency for a coupling grating. Radiation propagating in this direction was diffracted by the coupling grating to provide coupling between the lasers. Although emission at the other angles (where the interference pattern could be seen) was not diffracted by the grating, the interference pattern indicates that the light emitted by the two diode lasers was coherent with stationary locked phases. This thus shows that two separated lasers, coupled by a PTR Bragg grating, can behave as a single coherent source of light. The interference pattern, which was stable for hours of continuous operation, was the same during more than 11 months of repeatable experiments with the same two devices. In addition, the interference pattern had a visibility close to unity.

The reported results therefore show that a VBG could be used for efficient phase locking and coherent combining of two lasers. The next step was to design and study more complex VBGs with the potential of providing phase locking for a larger number of lasers. The proposed geometry for a scalable laser system is shown in Fig. 5. A thick reflecting Bragg grating is placed in front of a laser diode array [1] such that radiation from one of the side lobes is diffracted back to the adjacent emitter. To eliminate lasing of the low-order modes propagating along the axes of the individual emitters, we designed a new thick Bragg mirror with alternating stripes of high and low efficiency VBGs. Such a grating prevents back reflection of the radiation in front of each grating coupled surface emitting laser (GCSEL) and provides re-direction of the side lobes to the adjacent emitters in accordance with its spectral and angular selectivity.

An array of three broad area laser diodes with a periodicity of 1 mm was used in these experiments. A single emitter included a 1 mm-long active section with a 200 μm-wide stripe and a 0.75-mm-long internal grating output coupler. With external optical feed-back provided by a striped VBG placed at a distance of 2-4 mm from diodes, lasing in the form of two sets of side-

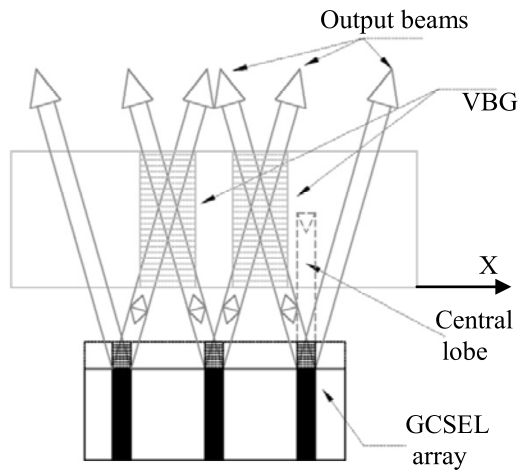

Fig. 5. Three-channel array of grating coupled surface emitting lasers (GCSELs) coupled by a striped reflecting volume Bragg grating (VBG).

lobe beams was observed above the threshold current density of 280 A/cm^2. The lasing wavelength of the coupled array was 976 nm and the spectral width was less than 70 pm Full Width at Half Maximum (FWHM). Phase-locking of the individual emitters in the array was confirmed by the far-field interference of the beams (Fig. 6).

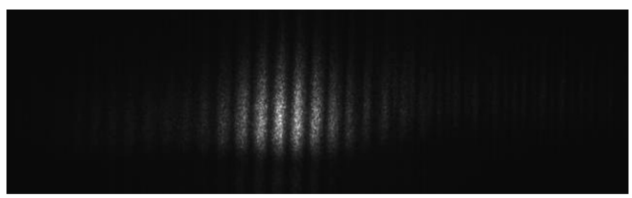

Fig. 6. Far field emission of a three-channel array.

With a pumping current of up to 1.5 times threshold, visibility of the interference pattern close to unity was observed. Therefore, all three GCSELs were phase locked and emitted coherent radiation. In addition, at this level of pumping, all three lasers which were originally multimode, emitted in a single transverse mode. At higher levels of pumping, a complex interference pattern of coherent multimode beams was observed. Finally, this result enables a new approach to multi-channel passive phase locking which can be used to increase the power of coherent emission from semiconductor and other types of lasers.

Therefore, the use of a single uniform VBG or multiple VBGs separated in space resulted in phase locking of different types of diode lasers. A similar approach was demonstrated for phase locking of fiber lasers [22]. Fig. 7 shows an experimental setup for coherent locking of two fiber lasers. This is referred to as the symmetrical architecture since the two lasers are symmetrically placed on the same side of the VBG. In this experiment, 3.3 m of Yb-doped panda-type polarization maintaining (PM) large mode area (LMA) fiber with a 25 µm core, a 250 µm cladding, and a birefringence of about 1.2×10^{-4} was used to construct each channel. Two 915 nm laser diodes having a maximum output power of 6 W were used to pump each channel through a (6+1)x1 PM high-power pump-signal combiner. Fibers in both channels were loosely coiled into a diameter of >12 cm and all fiber ends are angle cleaved to 6^{o}. The beam splitting VBG had a peak diffraction efficiency of ~ 50% and spectral selectivity of ~ 90 pm (FWHM) at an angle of incidence angle of approximately 4 degrees.

The output of each laser in Fig. 7 is incident at a small angle on the VBG and is partially diffracted and coupled into the other channel, thus creating a common cavity which effectively locks the two channels together. The spectral selectivity of the VBG provides strong mode selection and spectral narrowing of the output signal. Both lasers were operating at 1062.92 nm and emitted identical narrow lines which could not be resolved by the optical spectrum analyzer.

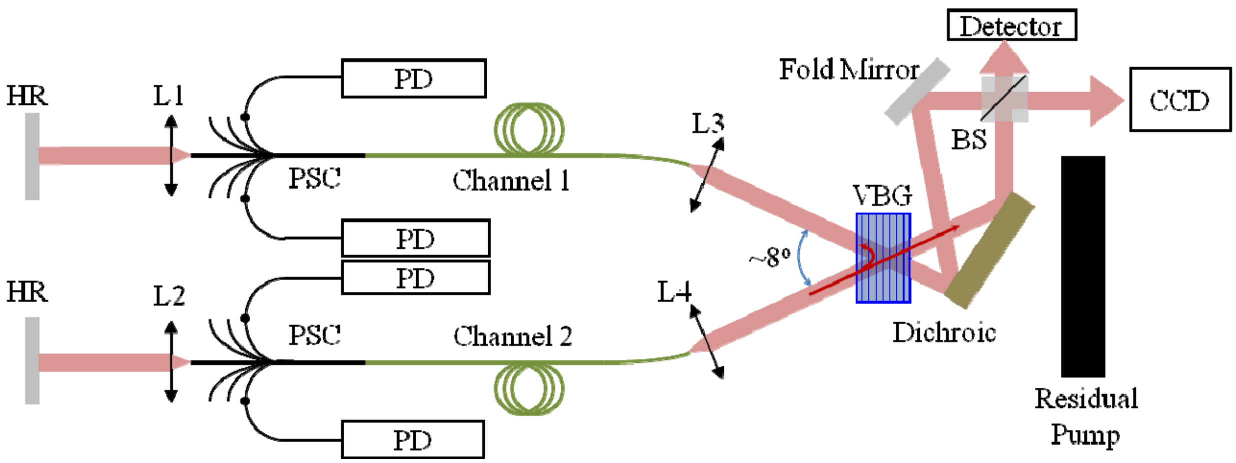

Fig. 7. Experimental setup for coherently locking two fiber lasers with a beam splitting VBG in the symmetrical configuration. L1, L2, L3, L4: f = 8 mm 0.5 NA aspheric lens; BS: beam splitter; PD: 915 nm pump diodes; PSC: (6+1)x1 pump-signal combiner.

However, spectral measurement with a Fabry-Perot scanning interferometer revealed a number of longitudinal modes oscillating under an envelope of 2.5 pm FWHM. The two output signals were interfered using a beam splitter cube and the interference fringes were observed with a charge coupled device (CCD) camera. The maximum contrast was about 96% with an average contrast of about 67%. This indicated a significant but not an ideal degree of coherence between the two beams. A combining efficiency of >80% was measured with respect to individual laser outputs and the maximum combined power was pump-limited to ~4 W.

In the previous paragraph, we demonstrated coherent locking of 2 fiber lasers using a single beam splitting VBG. In general, multiple VBGs can be recorded in the same PTR glass sample to realize a 1:N splitter/combiner. Fig. 8 (a-c) shows 1:2, 1:4, and 1:8 multiplexed VBG (M-VBG) splitters realized by recording 2, 4, and 8 identical high diffraction efficiency VBGs symmetrically in the same PTR glass sample [22]. Using a 1:N splitter, N channels can be coherently locked by a single element to obtain a coherent narrow linewidth, diffraction limited output. Note that in such a scheme, there is direct, equal radiation exchange between each fiber laser and locking is achieved using a single element.

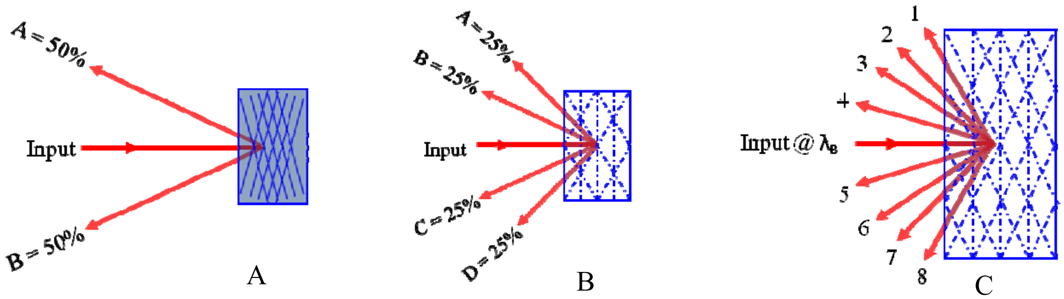

Fig. 8. Multiplexed VBG beam splitter: (A) 1:2 M-VBG splitter. (B) 1:4 M-VBG splitter. (C) 1:8 M-VBG splitter

Two symmetric VBGs were recorded in a single PTR glass sample at angles of +/- 3.3^o relative to the sample surface. Each VBG has a high peak diffraction efficiency (~ 99%) and a FWHM bandwidth of 210 pm. For a design wavelength around 1064 nm, this acts as a 50:50 beam splitter. The reflected beams make an angle of +/- 9.6^o in air relative to the input beam. By reversing the rays in Fig. 8 A, it is evident that two coherent beams A and B incident on the M-VBG element at an angle of +/- 9.6^o will be combined into a single beam normal to the M-VBG element.

Coherent locking of two fiber lasers was demonstrated using this 2nd order M-VBG splitter. The output radiation from the two fiber lasers was incident on the M-VBG at an angle of +/- 9.6^o in air. The mutually coherent part of the radiation that also satisfied the Bragg condition was diffracted towards the output coupler (80% reflective mirror at 1064 nm). The combined reflected radiation from the output coupler was split almost equally by the M-VBG for feedback to the two fiber lasers. A single coherent output was obtained through the output coupler. A small portion of coherent emission was also transmitted by the M-VBG and was used to make measurements. Fig. 9 left shows the emission spectra of the two channels (limited by spectrometer resolution). As in the previous cases, the two output signals were interfered to observe coherence fringes, see Fig. 9 right.

The results described above show that VBGs can be used for phase locking and coherent combining of both semiconductor and fiber lasers. To enable coherent combining of multiple laser sources, development of multiplexed VBGs that can split or combine several beams in the same volume is necessary. Prior to the work associated with this project, the state of the art was the incorporation of two VBGs in the same glass plate. The challenge associated with the current project is to develop a technology for recording multiple gratings in the same volume of PTR glass.

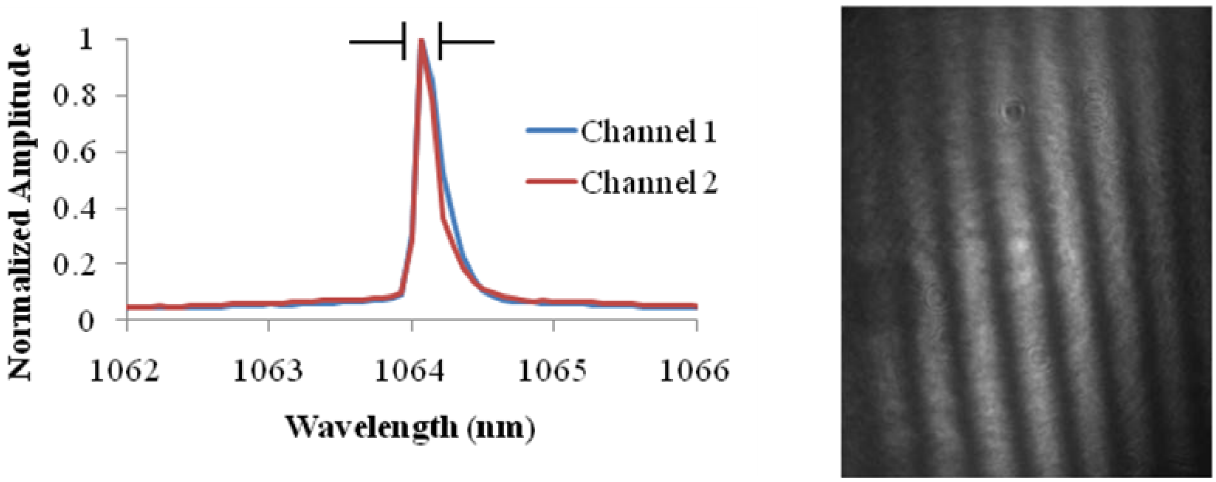

Fig. 9. (left) Emission spectra (limited by the spectrometer resolution) and (right) fringe pattern of the two channels for coherent locking using 2nd order M-VBG.

3. METHODS, ASSUMPTIONS AND PROCEDURES

To enable better quality VBG's for coherent beam combining, we improved the recording setup by adding an in-situ control of UV beam collimation after each beam expander by means of two shearing interferometers. This allows the shape of the interference fringes to be observed with a UV visualizer and the detection of collimation errors prior to exposure. To enhance the accuracy of the positioning of the PTR glass wafer during UV exposure, one branch of the recording setup involved a back-reflecting interferometer based on a He-Ne laser.

Figure 10 shows the schematic of the recording setup which enabled three-dimensional positioning of the PTR glass wafer simultaneously with recording. Beam quality was monitored by an interference pattern on a lateral screen. All optical elements were tested for high stability and the quality of the collimated UV beam was assessed by means of a Michelson interferometer. The recording setup provided UV beam stability of better than λ/2 at 325 nm during recording of the volume Bragg gratings.

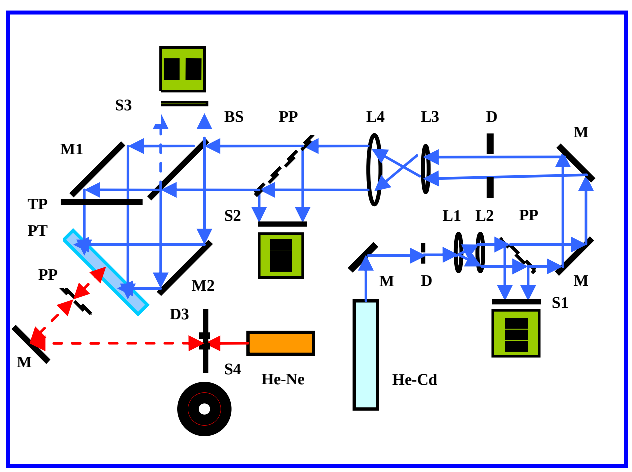

Fig. 10. Schematic of the holographic recording setup. He-Cd - UV laser at 325 nm, M - mirrors, D - diaphragms, L - lenses, PP – plane-parallel plates, S - screen, BS - beam splitter, PT –glass sample, TP – object projecting mirror, He-Ne – Vis laser at 633 nm.

The recording setup was further improved through the creation of a modular enclosure around the holographic table. A ~ 800 ft^3 enclosure with two "ENVIRCO-MAC-10-IQ" HEPA filters units was built to provide purified air to minimize the optical noise produced by diffraction of the UV laser beam on the dust particles during holographic recording. This enabled fabrication of high efficiency VBG elements for high density spectral beam combining.

To provide the highest possible efficiency and the narrowest selectivity at low absorption and scattering levels in the VBG elements, the multi-step thermal development procedure of VBG's was optimized. After each thermal development step, the diffraction efficiency was measured to enable determination of the evolution of the refractive index modulation and induced losses. Multiple thermal developments were performed at temperatures between 480 and 505°C.

A testing setup for both angular and spectral scanning was developed by introducing high-quality collimators into the laser probe beam. Additionally, a single-mode optical fiber was used as a spatial filter to improve the laser beam quality. The probe beam was focused into a single-mode fiber that was coupled with a second collimator. The resulting divergence of the probe beam was ~0.1 mrad. For the testing of reflecting VBG's (RBG's), a tunable laser (model Velocity 6320, New Focus) with a linewidth less than 300 kHz was coupled to an adjustable collimator to improve the quality of the beam to a level close to the diffraction limit. This enabled mapping of large-aperture VBG elements. The testing setup allowed simultaneous collection of data from two channels for transmitted and diffracted power. An optical spectrum analyzer (ANDO AQ 6317B) with ~10 pm spectral resolution was used for spectral measurements of a diffracted beam from a wide-spectrum source. RBG's having a FWHM spectral selectivity within the range of 75-220 pm were tested. No unexpected changes in the spectral selectivity related to the multi-step thermal development were observed. Nevertheless, it was found that Kogelnik's coupled-wave theory for thick holograms was limited by ~ 75 pm of FWHM spectral selectivity for thick (> 8 mm) VBG's. This limit was confirmed by an angular test of the same gratings using a tunable laser (Sacher Lasertechnik, TEC 500) with an emission linewidth less than 500 kHz.

During this project, several new techniques for manufacturing VBGs were developed. To improve the quality of large aperture VBG's, a new recording cell was designed to avoid backside reflections and UV light scattering from the dust particles. The recording procedure for large aperture VBG's was adjusted by taking into account peculiarities of UV beam propagation throughout the cell structure which consisted of thick fused silica windows as well as throughout the matching liquid. A calibration factor for this setup, which consisted of coherent UV beams illuminating the sample from the opposite sides, was determined by computer modeling of the beam propagation. Angular and spectral selectivity were measured to determine the diffraction efficiency and the corresponding refractive index modulation. It was demonstrated that a RBG could be recorded in the new cell with a diffraction efficiency as high as 98% and a FWHM spectral selectivity as low as 160 pm.

Finally, the plane of polarization of the incident laser beams on the PTR sample was rotated 90 degrees by a half-wave plate. Since the object beam projecting mirror was placed at less than 0.9 mm from the PTR glass plate, minimization of the phase distortions of the interfering UV beams by thermal disturbances of the air was accomplished. A matching liquid was also used to enable recording of high quality RBG's. In addition, the first and second exposure durations was optimized. By sequential thermal development, complex RBG elements with diffraction efficiencies of 90-93% were made with a slant angle accuracy of about 0.02 degrees.

4. RESULTS AND DISCUSSION

As part of this project, two prototype beam combiners were manufactured. The first prototype was recorded to explore the novel type of multiplexing, i.e., 5 volume Bragg gratings simultaneously in one piece of PTR glass. It was found that the holographic setup at OptiGrate Corporation enabled recording of multiplexed gratings in the same volume with similar efficiency. A special alignment procedure was developed to enable recording of multiple Bragg gratings having a degenerate Bragg angle. The fabricated gratings were positioned in the PTR glass with an accuracy of about 0.02°. The following specifications for the output angles were set for the first prototype in a beam splitting mode: -10.0 ± 1.0°, -5.0 ± 1.0°, 0.0 ± 1.0°, 5.0 ± 1.0°, 10.0 ± 1.0°. It should be noted that the "output angles" for beam splitting mode will correspond to the "input angles" when in beam combining mode. Also, the "input angle" in beam splitting mode will correspond to the "output angle" in beam combining mode. Parameters of the first prototype in beam splitting mode are summarized in Table 1.

Upon examination of Table 1, one can see that each multiplexed grating has an identical degenerate Bragg (input) angle of -0.04 degrees, while the output angles fit the specification with accuracy of 0.2°.

Table 1 – Parameters of the first prototype in beam splitting mode

Item Type	MTBG			
Part ID	N38-01			
Grating	I	II	III	IV
RWave, nm	1064	1064	1064	1064
Period, µm	6.13	12.21	12.24	6.14
Tilt, deg	-3.38	-1.71	1.65	3.32
Input Angle (at RWave), deg.	-0.04	-0.04	-0.04	-0.04
Output Angle (at Rwave), deg.	-10.20	-5.04	4.94	9.93
Measured ADE at 1064 nm, %	24.3	22.5	20.1	23.6
Thickness, mm	4.11			
Material losses, %	1			
Reflectivity per surface(1064 nm), %	<0.2			
Flatness, 633 nm	0.19; 0.16			
Grating dimensions, mm	25 x 25			

Parameters of the second prototype were adjusted for more convenient operation while more strict specifications on angular position of the gratings were set to ensure coherent combination. Table 2 presents the parameters of the second prototype.

Table 2. Parameters of the second prototype in beam splitting mode

Item Type	MTBG			
Part ID	N43-20			
Grating	I	II	III	IV
RWave, nm	1064	1064	1064	1064
Period, μm	6.35	6.36	12.61	12.67
Tilt, deg	3.24	-3.19	1.63	-1.58
Input Angle (at RWave), deg.	0.03	0.03	0.03	0.03
Output Angle (at Rwave), deg.	9.65	-9.57	4.85	-4.76
Measured ADE at 1064 nm, %	21.0	24.0	21.6	24.0
Measured ADE at 0.03° input angle, %	18.8	16.8	20.7	20.0
Transmittance at 0.03° input angle, %	23.3			
Thickness, mm	4.3			
Material losses, %	0.5			
Reflectivity per surface(1064 nm), %	<0.3			
Flatness, 633 nm	0.14λ; 0.13λ			
Grating dimensions, mm	22 x 22			

One can see that multiplexed gratings of the second prototype were embedded in a PTR glass wafer with an angular error for input angles of less than 0.05°. The diffraction efficiency of each grating is nearly identical within +/-2%. It was found that fine adjustment of the input angle for the beam splitting mode is required in order to achieve identical diffraction efficiencies for each channel. The measured diffraction efficiency in the beam splitting mode is shown in Fig. 11.

The incident beam, which is launched from the degenerate Bragg angle (to within 0.03°), is split into five beams. Four beams are diffracted by four multiplexed gratings into specified angles, while the fifth beam is formed by a residual beam in the transmitting channel. In beam combining mode, the element is operated in reverse with all five coherent beams being directed into the grating from the output angles. The combined output will emerge in the direction of the transmitting channel (degenerate Bragg or input angle). It is necessary to mention that this holographic element does not result in deterioration of the quality of the beams in any of the channels. Figure 12 shows the profiles of each of the split beams.

One can see that the beam profiles are nearly identical without visible distortions. Thus, it is expected that coherent combination will occur when five beams having diffraction limited beam quality are launched into a multiplexed hologram.

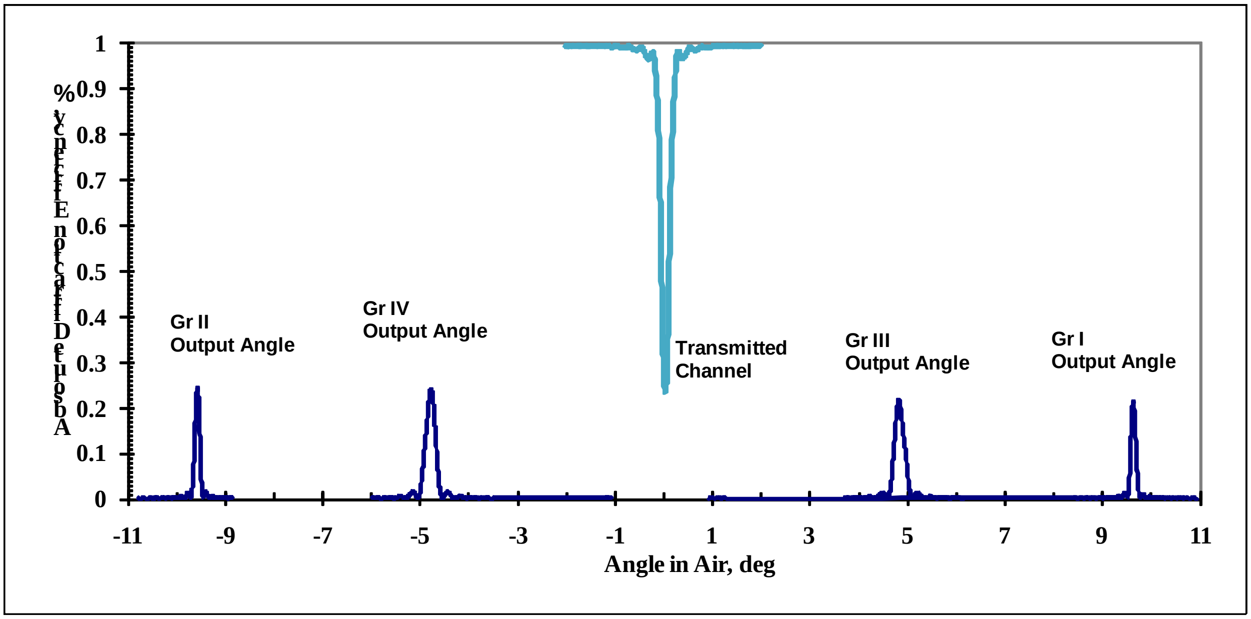

Fig. 11. Angular profile of multiplexed Bragg grating

In order to obtain good performance with high power beams, PTR glass having reduced absorption was chosen for manufacturing of the second prototype. The specially designed test station, shown below, was used for certification of absorption. A value of about 2×10^{-4} cm^{-1}

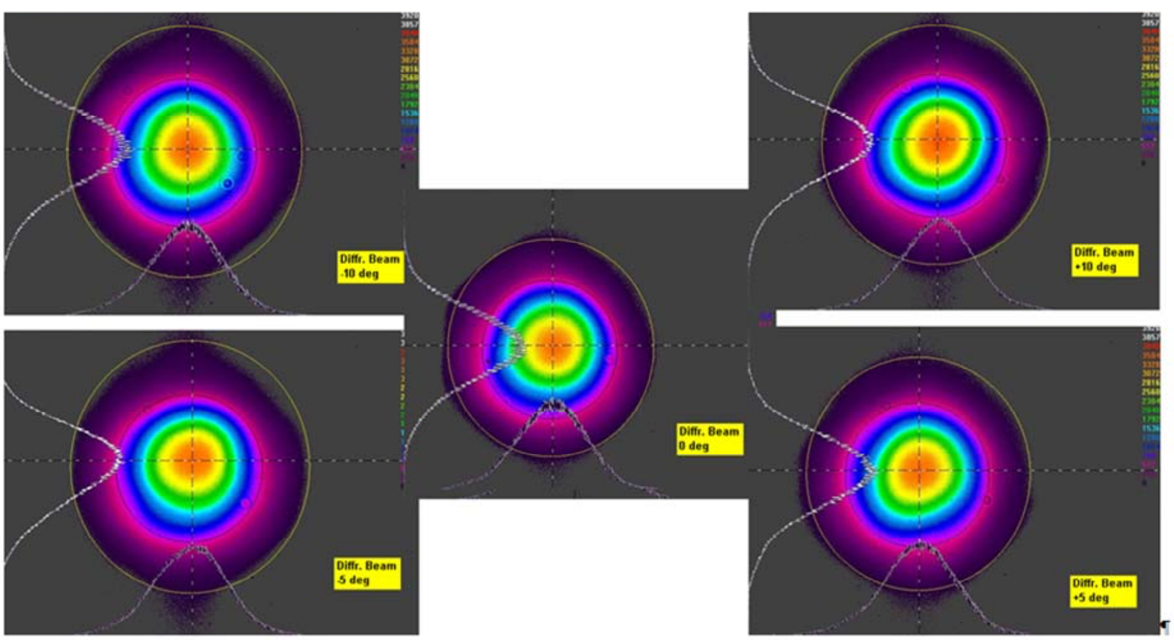

Fig. 12. Intensity distribution of each of the split beams

should enable operation of this element in high power beams. Please note that this element should not be exposed to UV radiation. Results of the measurements of the absorption in a multiplexed volume Bragg gratings for coherent beam combining are listed below.

The method used for measurement of the absorption in volume holographic elements recorded in PTR glass with ID# N36-39 is based on a pump/probe configuration that measures the changes in optical thickness of the glass plate during the laser induced heating. The setup used for this measurement is presented in Fig. 13. Two lasers were utilized: a He-Ne laser operating at 633 nm used as a probe laser, and a high power Yb-doped fiber laser used as the pump laser. A fraction of the probe beam is reflected by a fused silica wedge to a silicon photodiode to measure the probe power fluctuations while its main fraction is transmitted and overlapped with the pump laser beam in the plane of the sample.

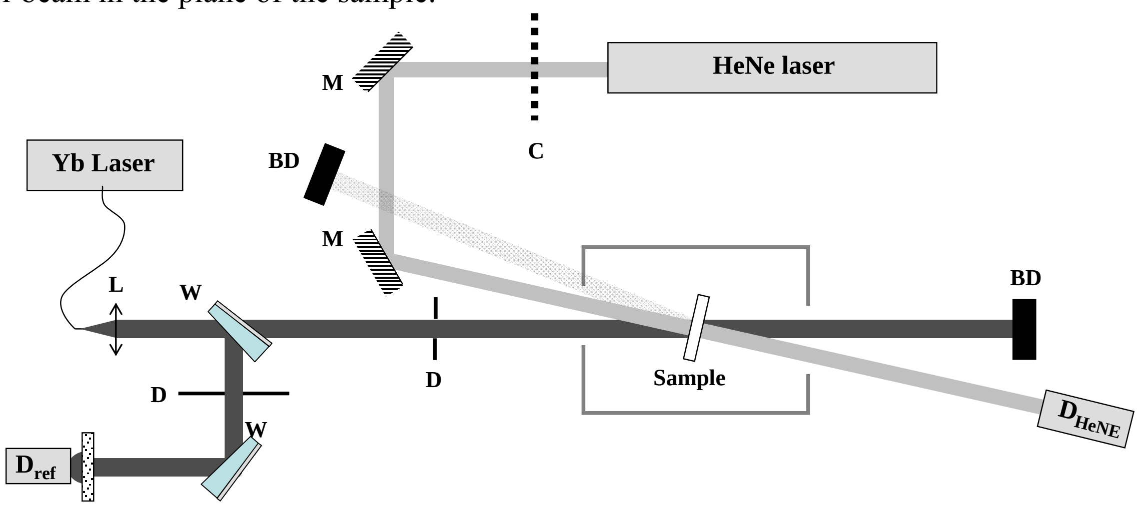

Fig. 13. Optical setup for the measurement of the phase shift induced by laser heating in an optical flat. W: wedge, L: lens, D: diaphragm, D_i: detector, M: mirror, C: chopper, and BD: beam dumps.

The angle between the two beams was set to ~4 degrees in order to secure an overlap of the two beams throughout the sample's thickness. The diameter of the probe beam is equal to 1 mm (FWHM) while the pump beam has a diameter of ~4 mm (FWHM). With these conditions, the probed area of the sample can be considered to be homogeneously heated by the high power radiation. After passing through the sample, the pump beam is sent to a beam dump while the probe laser beam is sent to a silicon detector to measure variations of the transmitted power which will follow an Airy function. These variations are then recalculated in terms of a change of the optical thickness and compared with the relative change of the optical thickness measured with a calibrated sample in order to extract the absorption coefficient of the sample. In this setup, pump power can be set to values as high as 100 W. In addition, absorption coefficients as low as 10^{-5} cm^{-1} can be measured. The relative precision is independent of the measured level of absorption and is better than 10%.

Using this method, absorption at 1085 nm was measured in the multiplexed grating after antireflection (AR) coating. It was supposed that absorption is uniformly distributed in the tested sample. The natural absorption coefficient, $\alpha(\lambda)$, is defined for a scattering-free medium as:

$$\alpha(\lambda) = \frac{-\ln(T(\lambda))}{t} \tag{1}$$

where $T(\lambda)$ is the fraction of transmitted power at wavelength λ and t is the sample thickness. The measured absorption coefficient after AR-coating was found to be equal to $(2.7 \pm 0.2)\times10^{-3}$ cm^{-1} and was too high for high power applications. An estimation can be made of the effect of such an absorption on the expected shift of the Bragg wavelength. It can be shown that with such an absorption, the estimated temperature increase of the VBG when illuminated by a 100 W beam at 1 μm would be equal to about 18^{o}C and would therefore result in a change of the Bragg wavelength by about 180 pm. In order to further decrease absorption, bleaching was performed by scanning a focused beam of the second harmonic of a Nd:YAG laser. Using this technique, absorption was decreased down to 10^{-3} cm^{-1}. An increase in the bleaching dosage permitted a further decrease of the absorption down to 7×10^{-4} cm^{-1}. At this level of absorption, the estimated temperature increase of the VBG when illuminated by a 100 W beam at 1 μm would be equal to less than 5^{o}C.

Finally, in order to confirm that the grating will behave the same at different power levels, we measured the absorption (which is related to heating) for different levels of pump power from 17 to 84 W (Table 3). No large fluctuations of absorption were noticed, i.e. heating of the gratings increased linearly with the level of pump power.

Table 3. Measured absorption in the N36-39 multiplexed VBG at 1085 nm

Pump power	17 W	34 W	50 W	67 W	84 W
Measured absorption, cm^{-1}	7.79E-04	7.06E-04	6.96E-04	7.06E-04	6.93E-04

5. CONCLUSIONS

A compact beam combiner based on multiplexed volume Bragg gratings (VBGs) is recorded in photo-thermo-refractive (PTR) glass. Five VBGs were multiplexed in a PTR glass wafer such that a common (degenerate) Bragg angle at the specified wavelength of 1064 nm was enabled. This element provides efficient superposition in the near and far fields of five coherent beams. The combiner was tested in the splitting regime and has shown full correspondence to specifications.

6. RECOMMENDATIONS

The optical parameters of the developed volume Bragg beam combiner are similar to those demonstrated with the Northrop-Grumman surface holographic element. An important feature of the volume beam splitter/combiner is that there is no complex surface profile that would be very sensitive to contamination. Further testing of this element in different configurations for beam splitting and combining along with multichannel fine spectral filtering is recommended.

7. REFERENCES

1. Oleksiy Andrusyak, Vadim Smirnov, George Venus, Vasile Rotar, and Leonid Glebov. Spectral Combining and Coherent Coupling of Lasers by Volume Bragg Gratings", IEEE J. of Selected Topics in Quantum Electronics, 15 (2009) 344-353.
2. P. Crump, W. Dong, M. Grimshaw, J. Wang, S. Peterson, D. Wise, M. DeFranza, S. Elim, S. Zang, M. Bougher, J. Peterson, S. Das, J. Bell, J. Farmer, M. DeVito, R. Martinsen, "100-W+ Diode Laser Bars Show >71% Power Conversion from 790-nm to 1000-nm and Have Clear Route to > 85%", Proc. of SPIE 6456, 645660M (2007).
3. Matthew Peters, Victor Rossin, Matthew Everett, and Erik Zucker, "High-power, high-efficiency laser diodes at JDSU", Proc. SPIE 6456, 64560G (2007).
4. M. Kanskar, T. Earles, T.J. Goodnough, E. Stiers, D. Botez, and L.J. Mawst, "73% CW power conversion efficiency at 50 W from 970 nm diode laser bars", Electron. Lett. **41**, 245 (2005).
5. L.B. Glebov, V.I. Smirnov, C.M. Stickley, I.V. Ciapurin, "New approach to robust optics for HEL systems" in Laser Weapons Technology III. W.E. Tompson and P.H. Merritt, Editors. Proceedings of SPIE 4724, 101-109 (2002).
6. L.B. Glebov, "Photosensitive glass for phase hologram recording," Glass Science and Technology, 71C (1998) 85-90.
7. L.B. Glebov, "Volume hologram recording in inorganic glasses," Glass Science and Technology 75 C1 (2002) 73-90.
8. O.M. Efimov, L.B. Glebov, V.I. Smirnov, and L.N. Glebova, "Process for production of high efficiency volume diffractive elements in photo-thermo-refractive glass," U.S. Patent 6,586,141 (2003).
9. O.M. Efimov, L.B. Glebov, and V.I. Smirnov, "High efficiency volume diffractive elements in photo-thermo-refractive glass," U.S. Patent 6,673,497 (2004).
10. Leonid Glebov, "Fluorinated silicate glass for conventional and holographic optical elements," Window and Dome Technologies and Materials X, edited by Randal W. Tustison, Proc. of SPIE Vol. 6545, 654507, (2007).
11. A.F. Glova, "Phase locking of optically coupled lasers," Quantum Electronics **33**, 283-306 (2003).
12. J. P. Hohimer, A. Owyoung, and G. R. Hadley, "Single-channel injection locking of a diode-laser array with a CW dye laser," Appl. Phys. Lett., **47,** 1244–1246 (1985).
13. J. Mercier, M. McCall, "Stability and dynamics of an injection-locked semiconductor laser array," Opt. Comm. **138**, 200-210 (1997).
14. A.P. Napartovich, D.V. Vysotsky, "The theory of radiation injection into a diode laser array," Opt. Comm. **141**, 91-98 (1997).
15. L. Bartelt-Berger, U. Brauch, A. Giesen, H. Huegel, and H. Opower, "Power-scalable system of phase-locked single-mode diode lasers," Appl. Opt. **38**, 5752-5760 (1999).
16. Y. Liu and Y. Braiman, "Synchronization of High-Power Broad-Area Semiconductor Lasers," IEEE J. of Selected Topics in Quantum Electronics, **10,** 1013-1024 (2004).
17. C.J. Chang-Hasnain, J. Berger, D.R. Scifres, W. Streifer, J.R. Whinnery, A. Dienes, "High power with high efficiency in a narrow single-lobed beam from a diode laser array in an external cavity," Appl. Phys. Lett. **50,** 1465-1467 (1987).
18. J.R. Leger, G. Mowry, and D. Chen, "Modal analysis of a Talbot cavity," Appl. Phys. Lett. **64**, 2937-2939 (1994).

19. S.Yu. Kourtchatov, V.V. Likhanskii, A.P. Napartovich, F.T. Arecchi, and A. Lapucci, "Theory of phase locking of globally coupled laser arrays," Physical Review A **52**, 4089-4094 (1995).
20. D. Sabourdy, V. Kermène, A. Desfarges-Berthelemot, L. Lefort, A. Barthélémy, P. Even, and D. Pureur, "Efficient coherent combining of widely tunable fiber lasers," Optics Express, **11**, 87-97 (2003).
21. George B. Venus and Armen Sevian, Vadim I. Smirnov, Leonid B. Glebov, "Stable coherent coupling of laser diodes by a volume Bragg grating in photothermorefractive glass," Opt. Lett. 31 (2006) 1453-1455.
22. Apurva Jain, Oleksiy Andrusyak, George Venus, Vadim Smirnov, Leonid Glebov. Passive coherent locking of fiber lasers using volume Bragg gratings. Proc. SPIE 7580 (2010) Fiber Lasers VII: Technology, Systems, and Applications, ed. K. Tankala, J.W. Dawson, 75801S 1-9.

DISTRIBUTION LIST

DTIC/OCP 8725 John J. Kingman Rd, Suite 0944 Ft Belvoir, VA 22060-6218	1 cy
AFRL/RVIL Kirtland AFB, NM 87117-5776	1 cy
Leanne Henry Official Record Copy AFRL/RDLA	1 cy